Elevated foraminifera-bound nitrogen isotopic composition during the last ice age in the South China Sea and its global and regional implications

Haojia Ren,[1,2] Daniel M. Sigman,[1] Min-Te Chen,[3] and Shuh-Ji Kao[4]

Received 15 December 2010; revised 7 November 2011; accepted 29 January 2012; published 24 March 2012.

[1] We report a new foraminifera-bound $\delta^{15}N$ (FB-$\delta^{15}N$) record from the South China Sea (SCS) extending back to 42 ka. This record shows a ~1.2‰ glacial-to-interglacial $\delta^{15}N$ decrease, with a deglacial $\delta^{15}N$ maximum similar to that observed in many bulk sedimentary $\delta^{15}N$ records and in a Caribbean FB-$\delta^{15}N$ record. The glacial-to-interglacial $\delta^{15}N$ decrease is smaller than in the Caribbean record, indicating that at least half of the Caribbean $\delta^{15}N$ decrease into the Holocene was regional, not global, supporting the interpretation of a Holocene increase in Atlantic nitrogen fixation. At the same time, the glacial-to-interglacial $\delta^{15}N$ decrease observed in the SCS may also be explained as a regional signal of increasing nitrogen fixation into the Holocene. Other aspects of the SCS record suggest an effect of physical circulation on FB-$\delta^{15}N$. FB-$\delta^{15}N$ starts to increase toward its deglacial maximum before the last ice age ends, and it continues to decrease through the later Holocene, in contrast to the more pure glacial/deglacial/interglacial steps in the Caribbean record. These changes have parallels in other Pacific $\delta^{15}N$ records, precessionally driven East Asian monsoon records, and the slow Holocene warming of SCS surface waters. In addition, the SCS record exhibits two one-point high-$\delta^{15}N$ spikes in multiple foraminiferal species that coincide with apparent hydrographic events. Thinning or weakening of the thermocline, in the late glacial and early Holocene as well as during the noted events, may have yielded a higher $\delta^{15}N$ for thermocline nitrate and thus a higher FB-$\delta^{15}N$.

Citation: Ren, H., D. M. Sigman, M.-T. Chen, and S.-J. Kao (2012), Elevated foraminifera-bound nitrogen isotopic composition during the last ice age in the South China Sea and its global and regional implications, *Global Biogeochem. Cycles*, *26*, GB1031, doi:10.1029/2010GB004020.

1. Introduction

[2] Biologically available, or fixed, nitrogen (N) is a critical nutrient for phytoplankton growth in most of today's ocean [*Dugdale and Goering*, 1967]. Temporal changes in the global inventory of fixed N could generate changes in the strength of the biological pump adequately large to contribute to the glacial-interglacial variations in atmospheric CO_2 [*McElroy*, 1983; *Falkowski*, 1997; *Altabet et al.*, 1995, 2002; *Ganeshram et al.*, 1995, 2002].

[3] The primary sources of fixed N to the ocean are terrestrial run-off, atmospheric deposition, and, most importantly, N fixation. The main sink is denitrification, in continental shelf sediments and the water columns of the eastern tropical North and South Pacific and the Arabian Sea. Sediment records from modern water column denitrification zones show clear N isotopic evidence of reduced water column denitrification during the last ice age relative to the current interglacial [*Altabet et al.*, 1995, 1999, 2002; *Ganeshram et al.*, 1995, 2002; *De Pol-Holz et al.*, 2006, 2007; *Robinson et al.*, 2007], and the sea level drop during the last ice age should have substantially reduced sedimentary denitrification [*Christensen*, 1994]. However, the history of fixed N inputs, especially N fixation, has proven more difficult to reconstruct. Our current understanding of the environmental regulation of N fixation has led to two major competing hypotheses for the glacial/interglacial changes in N fixation, one proposing a higher glacial N fixation rate due to higher dust flux and the release of N fixers from iron limitation [*Falkowski*, 1997; *Broecker and Henderson*, 1998] and the other arguing for a lower glacial N fixation rate as a response to lower denitrification rate in order to maintain a relative constant N:P ratio in the ocean [*Redfield*, 1958; *Schindler*, 1977; *Broecker*, 1982; *Tyrrell*, 1999; *Deutsch et al.*, 2004]. Reconstructing the history of global ocean N fixation changes over the recent glacial/

[1]Department of Geosciences, Princeton University, Princeton, New Jersey, USA.
[2]Now at Lamont-Doherty Earth Observatory, Palisades, New York, USA.
[3]Institute of Applied Geophysics, National Taiwan Ocean University, Keelung, Taiwan.
[4]Research Center for Environmental Changes, Academia Sinica, Taipei, Taiwan.

0886-6236/12/2010GB004020

interglacial cycles would not only clarify the strongest controls on N fixation but also have significant implications for changes in the ocean N budget and their carbon cycle impacts.

[4] The nitrogen isotopes of organic N preserved in sediments offer the potential to reconstruct past changes in N fixation. Presently, mean ocean nitrate δ^{15}N ($\delta^{15}N = {}^{15}N/{}^{14}N_{sample} / {}^{15}N/{}^{14}N_{reference} - 1$, the universal reference is N_2 in air) is around 5 ‰ [*Sigman et al.*, 2000] and is mainly controlled by the net isotope fractionation of global marine denitrification [*Brandes and Devol*, 2002; *Deutsch et al.*, 2004]. Isotope fractionation during N fixation is modest so that fixation introduces N with a δ^{15}N close to that of atmospheric N_2 (i.e., −2–0‰) [*Wada and Hattori*, 1976; *Montoya et al.*, 1992]. As a result, N fixation causes a regional decrease in the δ^{15}N of thermocline nitrate [*Karl et al.*, 2002; *Knapp et al.*, 2005, 2008]. The biomass produced in the surface incorporates nitrate supplied from below and/or newly fixed N. If well preserved in the sediments, the δ^{15}N of the organic matter may thus allow us to study changes in N fixation. However, the use of bulk sedimentary δ^{15}N in the low-productivity, low-latitude open ocean, where N fixation is thought to be focused, is normally compromised by bacterially driven degradation or terrestrial contamination [*Altabet and Francois*, 1994; *Schubert and Calvert*, 2001].

[5] In order to avoid these concerns, we have developed methods for the isotopic analysis of the organic N bound within the walls of planktonic foraminiferal tests [*Ren et al.*, 2009]. As this organic N is physically protected from diagenetic reactions and cannot be contaminated by detrital inputs, its δ^{15}N (foraminifera-bound δ^{15}N, or FB-δ^{15}N) may be an effective recorder of the δ^{15}N of N sources to the surface ocean in the oligotrophic regions. Measurements of modern surface sediments indicate that, the three euphotic zone dwelling, symbiotic, spinose species *Globigerinoides ruber*, *Globigerinoides sacculifer*, and *Orbulina universa* have a δ^{15}N similar to that of the new N supply to the euphotic zone [*Ren et al.*, 2009], which, in nutrient-depleted surface ocean regions, is set largely by the δ^{15}N of thermocline nitrate [*Altabet*, 1988; *Knapp et al.*, 2005]. The specific upper ocean processes that control FB-δ^{15}N are only now being investigated, but the similarity of FB- δ^{15}N among the euphotic zone dwellers can be rationalized in terms of their likely diet and their dinoflagellate symbionts [*Uhle et al.*, 1997; *Ren et al.*, 2012]. The FB-δ^{15}N of the deeper dwelling, non-spinose and/or asymbiotic species also correlates with, but is consistently higher than, the δ^{15}N of the thermocline nitrate [*Ren et al.*, 2012].

[6] A sediment record from the Caribbean Sea shows higher FB-δ^{15}N during the last ice age [*Ren et al.*, 2009]. Given that there is no evidence for such a large glacial-to-interglacial difference in mean ocean nitrate δ^{15}N [e.g., *Kao et al.*, 2008], the higher FB-δ^{15}N in the Caribbean Sea during the last ice age was interpreted as a regional reduction in N fixation rate [*Ren et al.*, 2009]. This evidence is supportive of a feedback between denitrification and N fixation, such that the ice age reduction in N fixation was due to global reductions in water column and sedimentary denitrification at that time [*Ren et al.*, 2009]. However, two issues remain to be addressed. First, the history of mean ocean nitrate δ^{15}N is a major uncertainty for this and other N isotope studies. To the degree that there has been a significant decrease in nitrate δ^{15}N since the last ice age, the data from the Caribbean would call for a correspondingly smaller change in Atlantic N fixation. Second, N fixation in the Atlantic is only a modest fraction of the global ocean rate [*Deutsch et al.*, 2007; *Knapp et al.*, 2008], so reconstructions of N fixation in other basins (e.g., the Pacific) are needed to understand the global N fixation response and to identify the environments in which different sensitivities and feedbacks apply.

[7] Bulk sediment δ^{15}N records from the South China Sea (SCS), a marginal sea in the western equatorial Pacific distant from the large denitrifying zones, have shown minimal changes over the last glacial/interglacial cycle, which was interpreted as evidence for a constant mean ocean nitrate δ^{15}N [*Kienast*, 2000]. However, this study has been disputed; for example, other sedimentary δ^{15}N records from an adjacent site show quite different features over the past 40 kyr [*Higginson et al.*, 2003]. While the inconsistency among bulk sediment records appears to arise from lateral sediment transport [*Kienast et al.*, 2005], one is still left with questions regarding the reliability of bulk sedimentary δ^{15}N as a recorder of sinking N δ^{15}N, in this region as elsewhere. Furthermore, the modern SCS and surrounding regions appear to be characterized by relatively rapid N fixation [*Capone et al.*, 1997; *Wong et al.*, 2002; *Chen et al.*, 2003; *Wong et al.*, 2007; *Chen et al.*, 2008; *Shiozaki et al.*, 2010], which has been shown to lower the subsurface nitrate δ^{15}N relative to the deep nitrate δ^{15}N [*Liu et al.*, 1996; *Wong et al.*, 2002]. Because of this and other processes, δ^{15}N changes in the N supply to the SCS euphotic zone cannot be assumed to derive solely from changes in mean ocean nitrate δ^{15}N. Indeed, it is arguably one of the best regions in the Pacific to use N isotopes to detect a regional change in N fixation.

[8] Here, we report a new FB-δ^{15}N record from South China Sea during the last 42 kyr. We interpret the data in context of the factors that affect the δ^{15}N of the nitrate supply to the euphotic zone of the South China Sea, which include mean ocean nitrate δ^{15}N, the regional N fixation rate, and the lateral and vertical communication of nitrate isotope signals by ocean circulation.

2. Study Area

[9] South China Sea (SCS) is the largest marginal sea in the world (Figure S1 in the auxiliary material) [*Sverdrup et al.*, 1942; *Chen et al.*, 2001], located in the tropical-to-subtropical western North Pacific.[1] The Luzon Strait between Taiwan and the Philippines is the principal deep channel allowing water exchange between the SCS and the western Pacific Ocean, whereas other channels (Taiwan Strait, Karimata Strait, and Mindoro Strait) are either too shallow or too narrow for effective water transport. The incoming North Pacific Tropical Water from the western North Pacific appears as a salinity maximum at around 150 m depth in the SCS [*Wong et al.*, 2007]. The North Pacific Intermediate Water (NPIW), which appears as a salinity minimum centered around 500 m in the SCS, can be traced to its source in the subpolar regions in the North

[1]Auxiliary materials are available in the HTML. doi:10.1029/2010GB004020.

Pacific [*You*, 2003; *Wong et al.*, 2007]. Deep water in the western North Pacific overflows the sill that separates it from the SCS at about 2200 m and fills the deep SCS. Consequently, the composition of deep water in the SCS is rather uniform and has characteristics similar to those in the western North Pacific at this depth [*Chen et al.*, 2006; *Wong et al.*, 2007]. During the glacial periods, when falling sea level exposed the broad shelves, the basin remained well ventilated and connected to the western North Pacific through the deep Luzon Strait [*Broecker et al.*, 1988, 1990; *Thunell et al.*, 1992]. Although the SCS was also connected to the Sulu Sea through Mindoro Strait during the glacial periods, the water transport today is mainly from SCS into Sulu Sea [*Chen et al.*, 2006] and was likely the same during the last ice age. In summary, the exchanges affecting the biogeochemistry of the SCS are dominated by the open western North Pacific.

[10] The surface circulation of the SCS changes seasonally in response to the monsoons. The northeastern monsoon, which prevails in winter and spring, forms a cyclonic gyre in the SCS, whereas the southwestern monsoon forms an anticyclonic gyre in summer and autumn [*Liu et al.*, 2002]. The monsoonal activity influences the nutrient dynamics and surface productivity of the SCS. The summer monsoon results in upwelling and enhanced primary productivity off the east coast of Vietnam, while the winter monsoon causes upwelling northwest of Luzon and north of the Sunda Shelf [*Liu et al.*, 2002]. Paleoceanographic records over the recent glacial cycles indicate higher export production associated with stronger winter monsoon in the northern basin, and with stronger summer monsoon in the southern basin [*Tamburini et al.*, 2003; *Wang et al.*, 2007]. It is thus unclear how the basin-wide thermocline should change in response to the precessionally driven ~20 kyr cycle in summer and winter monsoon strength.

[11] The surface water of the SCS is generally warm, stratified and oligotrophic. Both nitrate and phosphate concentrations in the mixed layer are typically below detection. New production at the surface is supported mostly by nutrients supplied from the subsurface [*Chen et al.*, 2004; *Chen*, 2005]. Nitrogen appears to be the primary limiting nutrient, rather than phosphorus, based on nutrient enrichment experiments [*Chen et al.*, 2004; *Chen*, 2005]. This N limitation may derive from the excess phosphorus in the lower thermocline: the water below 200 m in the northern SCS has a negative N* (N* = N−P + 2.90) and a δ^{15}N of around 6.2‰, higher than the mean deep ocean nitrate δ^{15}N, both of which suggest the communication of the signals of water column denitrification in the Eastern Tropical North Pacific (ETNP) across the Pacific by the vigorous lateral circulation [*Wong et al.*, 2002, 2007]. N fixation has been suggested to be an important source of fixed N to the SCS euphotic zone, in addition to the import of nitrate from below. Evidence for N fixation includes an increase in N* from depth to the subsurface by about 6 μM [*Wong et al.*, 2002, 2007], as well as relatively low subsurface nitrate δ^{15}N, which is as low as 4‰ in the north [*Wong et al.*, 2002], and 2.9–3.6‰ in and around the Vietnamese upwelling area [*Loick et al.*, 2007]. As a result of local and regional N fixation, the δ^{15}N of the sinking particles in the shallow sediment traps range from 2.7 to 4.5‰ across the basin [*Gaye et al.*, 2009], lower than the δ^{15}N of the lower thermocline nitrate, yielding an estimate of the contribution of N fixation to export production of around 9 to 14% [*Gaye et al.*, 2009]. Atmospheric deposition and riverine delivery also contribute fixed N to the basin, but their relative contributions are thought to be small relative to nitrate supplied from below and N fixation at the surface [*Wong et al.*, 2007]. Based on our current understanding of the N sources and dynamics in the SCS, we expect that the subsurface nitrate δ^{15}N in the SCS is sensitive to variations in local and regional N fixation, the lateral circulation that import N isotope signals from other regions in the Pacific, and the vertical circulation that affects the gradients in δ^{15}N across the thermocline.

3. Materials and Methods

[12] For this study, we focus on reconstructing FB-δ^{15}N during the last 42 kyr at site MD97–2142 (Figure S1 in the auxiliary material, 12°41′N, 119°27′E, water depth 1557 m), which was raised from the continental slope off Palawan Island during the 1997 IMAGES-III-IPHIS Cruise [*Chen and Beaufort*, 1998]. The sediments in this core are composed of light olive gray mud to foraminifera nannofossil ooze, interrupted by 18 visually distinguishable thin tephra layers. The bottom depth is well above the regional lysocline (~3500 m) [*Thunell et al.*, 1992], which ensures good carbonate preservation at this site. The sedimentation rate for the last 42 kyr is around 10 cm/kyr on average. We have sampled within one centimeter for every 10 cm.

[13] FB-δ^{15}N was measured on 6 common species in the >250 μm fraction, *Orbulina universa*, *Globigerinoides ruber, Globigerinoides sacculifer, Neogloboquadrina dutertrei, Globorotalia menardii*, and *Globigerinella aequilateralis*, as well as on mixed species of two size fractions, 250–355 μm and >355 μm. The protocol for measuring FB-δ^{15}N [*Ren et al.*, 2009] includes 1) chemical treatment of the foraminiferal shells to remove external N contamination, followed by acid dissolution of the cleaned shells, 2) conversion of organic nitrogen released into solution to nitrate by persulfate oxidation [*Nydahl*, 1978*; Knapp et al.*, 2005]; (3) measurement of nitrate concentration by chemiluminescence [*Braman and Hendrix*, 1989], and (4) bacterial conversion of nitrate to nitrous oxide [*Sigman et al.*, 2001], with measurement of the δ^{15}N of the nitrous oxide by automated extraction and gas chromatography-isotope ratio mass spectrometry [*Casciotti et al.*, 2002].

[14] Five to 10 mg of foraminiferal tests per sample were gently crushed, cleaned first by 5 min ultrasonication in 2% sodium hexametaphosphate (pH 8), then rinsed twice with deionized water (DI). To avoid any organic contamination associated with metal oxides, we conduct a reductive cleaning using sodium bicarbonate buffered dithionite-citrate reagent [*Mehra and Jackson*, 1958]. Samples were then soaked in 13% sodium hypochlorite (bleach oxidation) for 6 h, with several agitations to expose surfaces, and then rinsed five times with DI. The remaining 3 to 5 mg of cleaned foraminiferal tests were subsequently completely dissolved in 6 N hydrochloric acid, releasing organic matter for analysis. One Holocene sample and one glacial sample were selected to compare bleach oxidation with persulfate oxidation, the latter likely being a harsher treatment [*Brunelle et al.*, 2007]. These cleanings yielded indistinguishable N content and δ^{15}N, indicating

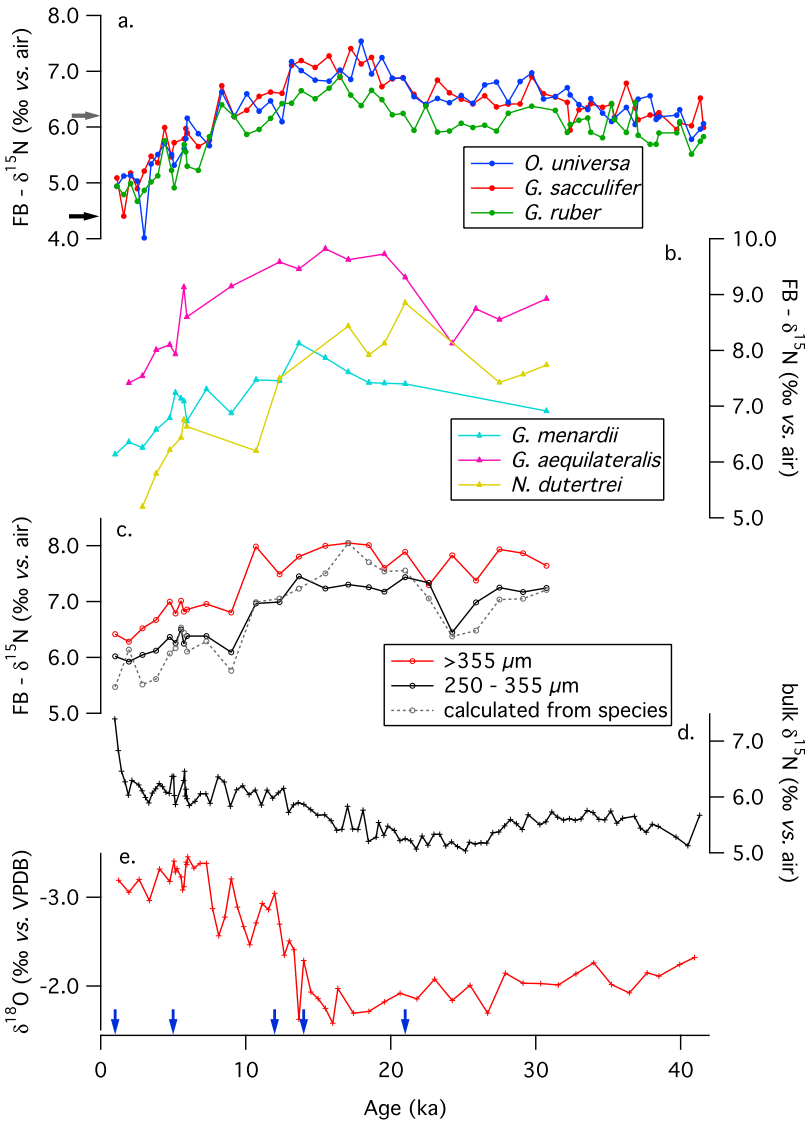

Figure 1. Planktonic foraminifera-bound δ^{15}N data. (a) Euphotic zone dwelling species. Blue: *O. universa*; Red: *G. sacculifer*; Green: *G. ruber.* Black and gray arrows indicate the δ^{15}N of present-day nitrate at 100 m and 300 m, respectively, in the northern South China Sea [*Wong et al.*, 2002]; the former approximates the nitrate supply to the euphotic zone while the latter represents the nitrate below the thermocline. (b) Sub-euphotic zone dwellers. Yellow: *N. dutertrei*; Light blue: *G. menardii*; Pink: *G. aequilateralis.* (c) Planktonic foraminifera-bound δ^{15}N of different foraminiferal size fractions, not picked for species. Red: >355 μm; Black: 250–355 μm; Grey dashed: weighted δ^{15}N for the 250–355 μm size fraction estimated from the 6 individual species in Figures 1a and 1b. In this calculation, when the δ^{15}N of a subsurface/thermocline species was not directly measured, we assumed the average δ^{15}N difference between the euphotic zone and sub-euphotic zone dwellers. (d) Bulk sediment δ^{15}N. (e) δ^{18}O of *G. ruber* (white) calcite (‰ v. VPDB) from *Wei et al.* [2003]. Blue arrows are calibrated radiocarbon dates.

complete removal of external contamination and confirming the physically protected nature of shell-bound N. Duplicates or triplicates were made for the full analytical protocol on cleaned foraminifera, yielding standard deviations (1 sigma) for FB-δ^{15}N of generally better than 0.2‰.

[15] The age model for core MD97–2142 was adapted from *Wei et al.* [2003] and is based on five AMS ^{14}C-dates, and the correlation of stable oxygen isotopes (*Globigerinoides ruber* sensu stricto, white, 250–300 μm) with the low-latitude oxygen isotope stack of *Bassinot et al.* [1994].

[16] The total N (TN), organic N (N_{org}) and organic carbon (C_{org}) contents as well as the isotopic composition (δ^{15}N and $\delta^{13}C_{org}$) were analyzed at MD97–2142. See auxiliary material for these methods, results and discussion.

4. Results

[17] The three euphotic zone-dwelling planktonic foraminiferal species (*O. universa, G. sacculifer, and G. ruber*) are characterized by a higher δ^{15}N during the last ice age (Figure 1a). Before 20 ka, δ^{15}N of *G. ruber* is stable around

6‰, while δ^{15}N of *O. universa* and *G. sacculifer* increase slightly toward the end of the Last Glacial Maximum (LGM), by about 0.5‰. The δ^{15}N of all three species increases after 20 ka by about 0.5–1.1‰, remains at this maximum during the early deglaciation, and then decreases across the late deglaciation and early to mid-Holocene. The glacial FB-δ^{15}N of the three species is close to modern deep nitrate δ^{15}N in the northern SCS (~6.2‰ below 250 m) [*Wong et al.*, 2002], as well as the nitrate δ^{15}N of the North Pacific Intermediate Water (NPIW) (~6.1‰) [*Liu et al.*, 1996]. The average FB-δ^{15}N in the surface sediments (the top 27 cm or between 1 and 2.53 ka) is 4.9‰, consistent among the three species, close to the subsurface nitrate δ^{15}N minimum measured at 100 m in the northern SCS (~4.4‰) [*Wong et al.*, 2002]. *O. universa* and *G. sacculifer* are similar throughout the record, especially after 3-point smoothing (Figure S2 in the auxiliary material). The δ^{15}N of *G. ruber* is slightly lower than the other species (Figure S2a in the auxiliary material); this difference is generally greatest between 16 and 25 ka (Figure S2b in the auxiliary material), roughly similar to what has been observed in the Caribbean, where the maximal species difference also occurs at the LGM [*Ren et al.*, 2009]. This suggests that a similar interpretation for the LGM differences as put forward for the Caribbean data may also apply to the SCS (Text S1 in the auxiliary material). However, the SCS data show smaller inter-species differences than observed in the Caribbean [*Ren et al.*, 2009], perhaps reflecting a less clear vertical structure within the euphotic zone in the SCS, as a result of stronger upwelling and weaker stratification (Text S1 in the auxiliary material). At approximately 8.3 ka, 5.8 ka, and 4.4 ka in our SCS record, there are three upward spikes in δ^{15}N appearing in all three euphotic zone dwelling species (Figure 1a).

[18] As observed previously, the δ^{15}N of the subsurface species *G. aequilateralis*, and two thermocline species, *G. menardii* and *N. dutertrei*, is consistently higher than that of the euphotic zone species (Figure 1b) [*Ren et al.*, 2009, 2012]. However, all species show similar trends, with higher glacial values, a maximum during LGM and early deglaciation, and decreasing δ^{15}N throughout the late deglaciation and the Holocene (Figure 1b).

[19] The six species contribute more than 60% of the planktonic foraminiferal shells in the sediments, and they are mostly picked from the 250–355 μm fraction. As a result, the δ^{15}N of the mixed species from the two 250–355 μm and >355 μm size fractions resembles the trends for individual species, and the $CaCO_3$ mass- and N content-normalized δ^{15}N calculated from the six species is remarkably consistent with the measured δ^{15}N of the 250–355 μm size fraction. The δ^{15}N of the >355 μm fraction is higher than that of the 250–355 μm fraction, probably due to higher abundance of subsurface and thermocline species in the larger size fraction (Figure 1c).

[20] Bulk sedimentary δ^{15}N shows almost the opposite trend as FB-δ^{15}N, with a lower glacial value of around 5.5‰, a higher Holocene δ^{15}N of around 6‰, and much higher δ^{15}N in the shallowest sediments (Figure 1d). Our FB-δ^{15}N record is drastically different from the bulk sedimentary δ^{15}N record at this site (Figure S3 in the auxiliary material) and from previous studies in the SCS [*Higginson et al.*, 2003; *Kienast et al.*, 2005], which adds to other concerns regarding the reliability of bulk sedimentary δ^{15}N in the SCS (Text S1 in the auxiliary material).

5. Interpretation and Discussion

[21] In the modern South China Sea much as in the western North Atlantic, the δ^{15}N of subsurface nitrate supplied to the euphotic zone is lower than that of the deep nitrate, apparently due to the input of newly fixed N [*Wong et al.*, 2002]. In a two-end-member mixing model, the subsurface nitrate δ^{15}N should equal the flux-weighted average δ^{15}N between N fixation and deep nitrate supply. The δ^{15}N of the subsurface nitrate may thus be affected by changes in the δ^{15}N of the deep nitrate supply, the regional N fixation rate, and the lateral and vertical communication of nitrate isotope signals by ocean circulation. We will discuss our FB-δ^{15}N record in the context of these factors and consider different scenarios that may explain the observed glacial/interglacial changes in the FB-δ^{15}N.

5.1. Difference in FB-δ^{15}N Between the LGM and the Late Holocene

[22] The FB-δ^{15}N of the three euphotic zone dwellers, *G. ruber*, *G. succulifer*, and *O. universa*, measured in the shallowest sediment (~4.8–5.1‰) is similar to the modern shallow subsurface nitrate δ^{15}N minimum in the northern SCS (~4.4‰) [*Wong et al.*, 2002] (Figure 1a). This is consistent with previous observations that FB-δ^{15}N of the euphotic zone dwellers is similar to the δ^{15}N of the N sources to the euphotic zone, which in the nutrient-deplete regions is set largely by the δ^{15}N of thermocline nitrate [*Ren et al.*, 2009]. We thus take FB-δ^{15}N of the euphotic zone dwellers to be controlled largely by past changes in subsurface nitrate δ^{15}N. Given the relationship between core top FB-δ^{15}N of the mixed layer dweller, *G. ruber*, and the modern subsurface nitrate δ^{15}N in the northern SCS [*Wong et al.*, 2002], the glacial *G. ruber* δ^{15}N (averaged between 21 and 29 ka) suggests a 1.2‰ higher subsurface nitrate δ^{15}N of 5.6‰, close to the present-day nitrate δ^{15}N of NPIW (Figures 1a and 2) [*Liu et al.*, 1996; *Wong et al.*, 2002].

[23] One possible interpretation of the ice age-to-late Holocene FB-δ^{15}N difference is that it derives solely from a change in mean ocean nitrate δ^{15}N. To estimate the change, we assume that thermocline nitrate δ^{15}N is determined by contributions of nitrate from only two sources: upward mixing of subthermocline nitrate (with a present-day δ^{15}N of 6.2‰) and the remineralization of newly fixed N to nitrate (with a δ^{15}N of −1‰). For the purposes of this calculation, we assume that these two contribute in the same proportion during the Holocene and LGM, and the δ^{15}N of the subthermocline or NPIW nitrate is primarily affected by changes in the mean ocean nitrate δ^{15}N. From these assumptions, the ice age-to-late Holocene *G. ruber* δ^{15}N change of 1.2‰ yields an ice age mean ocean nitrate δ^{15}N that is 1.6‰ higher than the Holocene value (Figure 2, in purple, and Figure 3a). The translation of the 1.2‰ foraminiferal change to a 1.6‰ mean ocean nitrate change derives from the calculation's removal of the isotopic dilution of shallow subsurface nitrate by the newly fixed N contribution.

[24] As described above, our previous FB-δ^{15}N record from the Caribbean Sea showed a similar but larger amplitude δ^{15}N decrease from the last ice age to the Holocene

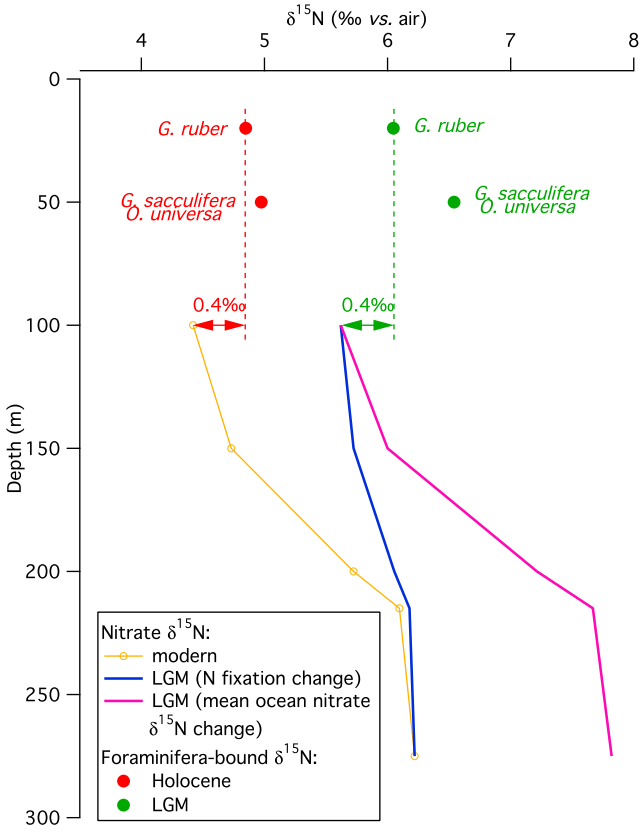

Figure 2. Depth profiles of nitrate δ^{15}N in the South China Sea as measured in the modern ocean and reconstructed for the last Glacial Maximum. Orange open circles: Average δ^{15}N of nitrate in the upper 300 m at the South East Asia Time series Station (SEATS, 18°N, 116°E, in the South China Sea) [*Wong et al.*, 2002]; the increase in nitrate δ^{15}N at the base of the euphotic zone, due to nitrate assimilation, is excluded. Red and green filled circles: average foraminifera-bound δ^{15}N during the Holocene and the LGM respectively. *G. ruber* lives shallower within the euphotic zone than the other two species, as supported by the lower carbonate δ^{18}O of *G. ruber* [*Lin and Hsieh*, 2007] and observed elsewhere [*Ravelo and Fairbanks*, 1992]. Blue and purple lines: proposed LGM depth profiles of nitrate in the thermocline considering only a change in N fixation rate (blue line) and only a change in mean ocean nitrate δ^{15}N (purple line), in both cases assuming a constant δ^{15}N difference between *G. ruber* and subsurface nitrate.

[*Ren et al.*, 2009]. Given the effect of N fixation to lower the δ^{15}N of shallow subsurface nitrate in the North Atlantic [*Knapp et al.*, 2008], the FB-δ^{15}N change was interpreted as indicating a deglacial increase in regional N fixation. If the Caribbean δ^{15}N change (of 1.8‰) were instead assumed to derive solely from a change in mean ocean nitrate δ^{15}N, the same calculation would suggest a δ^{15}N change of 3.1‰, roughly twice as great as that derived from the SCS data (Figure 3a). Thus, interpretation of the SCS record as a reconstruction of mean ocean nitrate δ^{15}N suggests that it could only explain half of the subsurface δ^{15}N change in the Caribbean Sea record, such that at minimum half of the observed glacial/interglacial δ^{15}N difference in the Atlantic record must result from a regional change in N fixation (i.e., the ice age Atlantic N fixation rate would be 62%, instead of 21%, of its Holocene rate; Figure 3a), strengthening the argument that N fixation in the N. Atlantic was significantly reduced during the last ice age.

[25] However, we have no reason to believe that mean ocean nitrate δ^{15}N change is the dominant signal recorded in our SCS FB-δ^{15}N record. In fact, a glacial increase in mean ocean nitrate δ^{15}N is unlikely. The widely observed decrease in water column denitrification [*Altabet et al.*, 1995, 1999, 2002; *Ganeshram et al.*, 1995, 2002; *De Pol-Holz et al.*, 2006, 2007; *Robinson et al.*, 2007] would have worked to lower the glacial nitrate δ^{15}N, requiring a proportionally similar (in detail, a slightly greater) decrease in sedimentary denitrification to prevent a whole ocean nitrate δ^{15}N decrease during the last ice age [*Brandes and Devol*, 2002; *Deutsch et al.*, 2004]. N fixation is the most likely driver of the first-order LGM-to-Holocene FB-δ^{15}N difference in the SCS. As in the Caribbean, the δ^{15}N of nitrate just below the euphotic zone in the modern SCS is lower than that of nitrate below the thermocline, due to the addition of newly fixed N [*Wong et al.*, 2002, 2007; *Loick et al.*, 2007]. Higher subsurface nitrate δ^{15}N during the last ice age could thus have reflected a reduction in N fixation rate within SCS and/or the western equatorial Pacific. Indeed, while late Holocene FB-δ^{15}N in the SCS is similar to the δ^{15}N of the shallowest subsurface nitrate measured in the modern SCS, ice age FB-δ^{15}N is similar to sub-thermocline nitrate δ^{15}N (Figure 2). The ice age-to-Holocene decrease in FB-δ^{15}N is smaller in the SCS than in the Caribbean by the same degree that the depression in the δ^{15}N of modern thermocline nitrate is smaller in SCS than in the Sargasso Sea. Assuming constant mean ocean nitrate δ^{15}N and thus a similar partitioning of N loss between sedimentary and water column denitrification during the last ice age and the Holocene [*Deutsch et al.*, 2004], the inferred change in subsurface nitrate δ^{15}N in the SCS suggests that the glacial N fixation rate in or near the SCS was ~27% of its late Holocene rate, again similar to the estimated reduction of N fixation in the subtropical N. Atlantic (Figure 3b). These coincidences make a compelling if circumstantial case that N fixation-driven changes of thermocline nitrate δ^{15}N may explain the LGM-to-Holocene FB-δ^{15}N difference at both sites.

[26] The mechanistic explanation for the ice age-to-Holocene increase in N fixation in the Atlantic was that greater Holocene denitrification rates reduced the N:P of the nutrient supply to Atlantic surface waters, which provided a competitive advantage for N fixers [*Ren et al.*, 2009]. Given the evidence for a regional influence of denitrification in SCS waters, this explanation applies equally well in the SCS. Although modern studies in the SCS suggest that N fixation may increase during winter/spring as a result of higher atmospheric iron deposition [*Wong et al.*, 2002, 2007], our data do not support iron availability as the primary control of N fixation over the last glacial/interglacial cycle, given the evidence for greater dust flux during the last ice age [*Winckler et al.*, 2008].

5.2. Deglacial FB-δ^{15}N Maximum

[27] The deglacial δ^{15}N maximum in the SCS record, that is about 0.5‰ higher than the average glacial value, is most likely to derive from changes in mean ocean nitrate δ^{15}N.

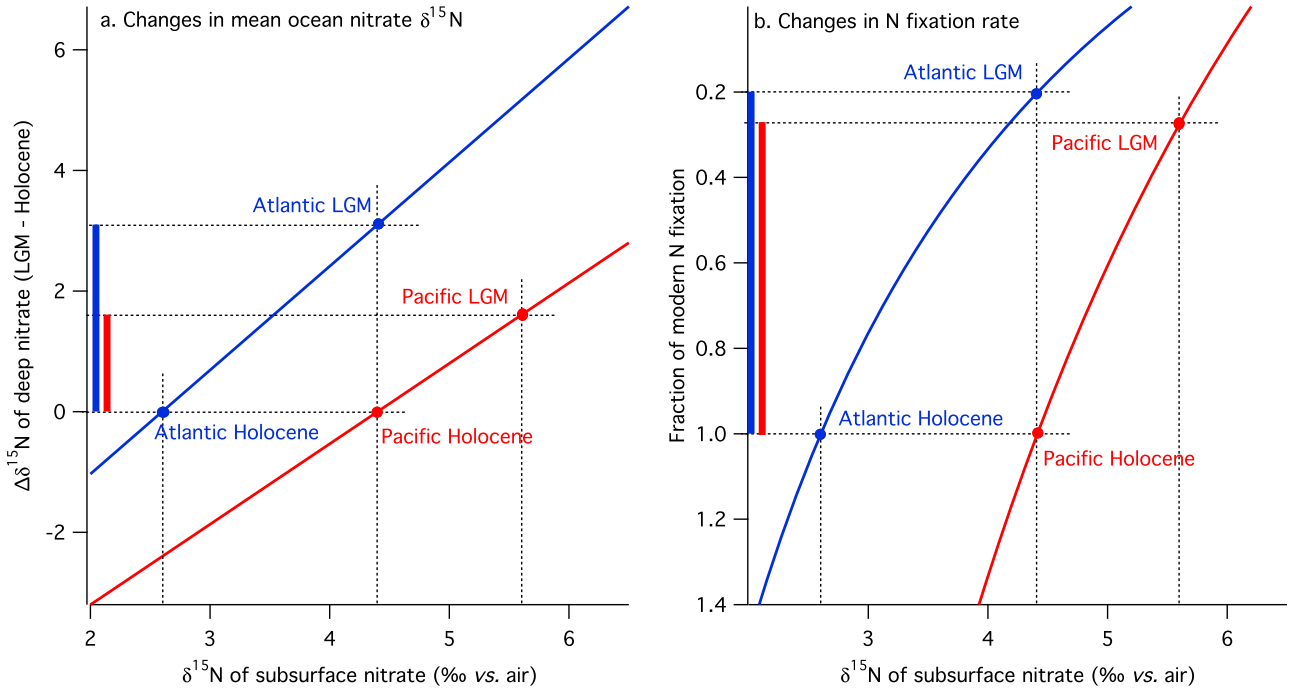

Figure 3. (a) Ice age-to-Holocene change in deep ocean nitrate δ^{15}N required to account for the observed changes in shallow subsurface nitrate δ^{15}N inferred from the FB-δ^{15}N record in the South China Sea (red) and the Caribbean (blue), assuming no change in N fixation and vertical mixing rate. (b) The fraction of N fixation rate relative to its Holocene value required to account for the observed changes in shallow subsurface nitrate subsurface δ^{15}N inferred from the FB-δ^{15}N record in the South China Sea (red) and the Caribbean (blue), assuming no change in mean ocean nitrate δ^{15}N and vertical mixing rate. All the calculations are based on a two end-member mixture of newly fixed N with a δ^{15}N of −1‰ [*Carpenter and Price*, 1977; *Montoya et al.*, 2002] and the deep thermocline nitrate with a δ^{15}N of 6.2‰ in the South China Sea (below 200 m at the SEATS [*Wong et al.*, 2002]) and 5.2‰ in the N. Atlantic (from 1000 m at the Bermuda Atlantic Time series Site [*Knapp et al.*, 2005]). The δ^{15}N of modern subsurface nitrate is 4.4‰ in the South China Sea [*Wong et al.*, 2002] and 2.6‰ in the N. Atlantic [*Knapp et al.*, 2005]. The calculated ice age subsurface nitrate δ^{15}N is 5.6‰ in the South China Sea, and 4.4‰ in the N. Atlantic, based on the ice age δ^{15}N of *G. ruber*, the species with the smallest LGM-Holocene change.

Many of the eastern Pacific records in the water column denitrification regions show δ^{15}N declines subsequent to the early deglacial rise associated with increase in the regional denitrification rate (Figure 4a) [*Altabet et al.*, 1995, 1999, 2002; *Ganeshram et al.*, 1995, 2000; *Robinson et al.*, 2007]. In the Caribbean Sea FB-δ^{15}N record as well as in a number of bulk sedimentary δ^{15}N records at regions away from the denitrification zones [e.g., *Kao et al.*, 2008] (black curve in Figure 4b), such a deglacial maximum is observed, in apparent synchrony with the deglacial increase in water column denitrification in the eastern Pacific [*Brunelle et al.*, 2007; *Galbraith et al.*, 2008], suggesting a global nitrate δ^{15}N maximum linked to deglacial changes in denitrification. Modeling results indicates that the early deglacial maximum in mean ocean nitrate δ^{15}N is likely to be driven mostly by a delay between increased water column denitrification and increased sedimentary denitrification, which produces a maximum in the water column to sedimentary denitrification ratio [*Deutsch et al.*, 2004].

5.3. Other Features of the SCS FB-δ^{15}N Record

[28] Figure 5 qualitatively summarizes our preferred interpretation presented above for the major features of the SCS FB-δ^{15}N record and highlights the aspects of the record that it has not yet addressed. In this interpretation, the δ^{15}N of NPIW nitrate is primarily influenced by changes in mean ocean nitrate δ^{15}N, which undergoes a deglacial maximum but does not change substantially between the last ice age and the interglacial (red line in Figure 5). N fixation is then the primary driver for the glacial/interglacial difference in δ^{15}N; the greater its amplitude, the more it depresses the SCS FB-δ^{15}N relative to mean ocean nitrate δ^{15}N (downward green arrows in Figure 5). The mean ocean nitrate δ^{15}N history and that of regional N fixation thus combine to yield a basic template for FB-δ^{15}N change (green line in Figure 5), to which the actual data are compared.

[29] There are at least three deviations from the template that deserve our attention (shown in blue shading in Figure 5). First, the δ^{15}N maximum that spans the deglacial interval begins surprisingly early at around 20 ka, 2–4 kyr prior to the deglaciation. Thus, an explanation is required for why SCS FB-δ^{15}N should increase before the well-documented water column denitrification increase between 18 and 14 ka (blue area prior to 18 ka in Figure 5). Second, SCS FB-δ^{15}N declines through the Holocene, rather than reaching a stable Holocene value as seen in the Caribbean

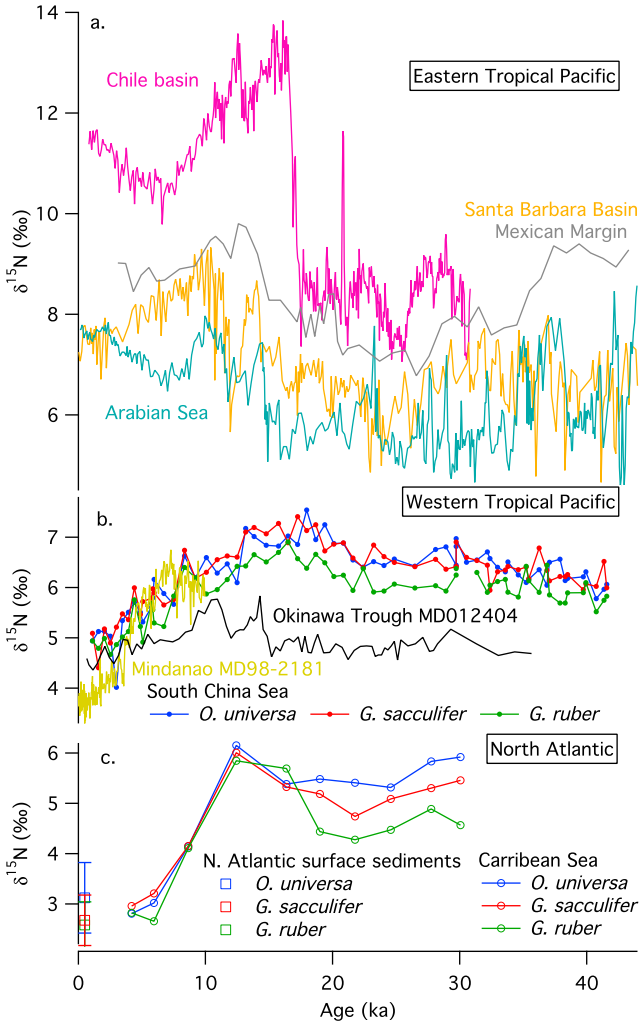

Figure 4. Global compilation of N isotope records since the last ice age. (a) Bulk sedimentary δ^{15}N records from each of the major water column denitrification zones: the eastern Pacific off Chile [*De Pol-Holz et al.*, 2006], the eastern tropical North Pacific (Santa Barbara Basin [*Emmer and Thunell*, 2000] and Mexican Margin [*Ganeshram et al.*, 1995]), and the Arabian Sea off Oman [*Altabet et al.*, 2002]. (b) δ^{15}N records from the western Pacific: MD97–2142 foraminifera-bound δ^{15}N record from the South China Sea (this study) and two bulk sedimentary δ^{15}N records, MD98–2181 from the western equatorial Pacific off Mindanao [*Kienast et al.*, 2008] and MD012404 from the Okinawa Trough [*Kao et al.*, 2008]. (c) Foraminifera-bound δ^{15}N records from ODP Site 999 in the Caribbean Sea, as well as from surface sediments at three other tropical N. Atlantic sites, near Barbuda Antiqua, Great Bahama Banks, and Little Bahama Banks (error bars indicate variations in FB-δ^{15}N among these three sites) [*Ren et al.*, 2009]. Note that we placed these data against the *y* axis at 0.5 ka; however, these sediments are undated.

FB-δ^{15}N record [*Ren et al.*, 2009] (Figure 4c). This appears as a positive deviation relative to the template in the Holocene (blue area after 14 ka in Figure 5), although a different choice for the interglacial N fixation template could have made this feature appears as a negative deviation in the late Holocene. Third, there are three upward spikes in δ^{15}N after 10 ka (upward spikes in the blue area in Figure 5). These occur in all three euphotic zone dwelling species (Figure 1a) and thus would seem to be "real" events requiring explanation. These δ^{15}N spikes are not cleanly distinguishable from the second observation made above, that of a surprisingly slow decline in δ^{15}N to its ultimate value in the late Holocene, except for the correspondence of two of these events with apparently climate-related changes in the δ^{18}O and species abundance of planktonic foraminifera (see below).

[30] It is plausible that denitrification in the eastern Pacific as well as local hydrographic changes have had stronger influences for FB-δ^{15}N in the SCS than at the site of our previous FB-δ^{15}N record in the Caribbean. While the Pacific denitrification regions are distant from the SCS, vigorous equatorial Pacific circulation communicates the biogeochemical and isotopic signals of denitrification across the basin [e.g., *Sigman et al.*, 2009; *Rafter et al.*, 2012]. The North Equatorial Current (NEC), which has an N deficit due to water column denitrification in the ETNP, serves as an important source of subsurface water in the western equatorial Pacific, and enters the SCS through the Luzon strait. The elevated δ^{15}N of subthermocline nitrate (6.2‰, compared to ~5.2‰ in the tropical North Atlantic) speaks to the influence of regional denitrification in the modern SCS and the potential for changes in circulation to introduce more or less of a denitrification signal into the basin.

[31] The continuous δ^{15}N decrease through the Holocene in the SCS seems to be a feature shared in a few bulk sedimentary δ^{15}N records from the western Equatorial Pacific off Mindanao [*Kienast et al.*, 2008] (yellow curve in Figure 4b). A Holocene drift in mean ocean δ^{15}N is certainly possible, even in the case that the ocean N budget has effectively reached steady state in terms of global ocean fixed N content [*Deutsch et al.*, 2004]. However, the Caribbean Sea FB-δ^{15}N seems to have leveled off after 8 ka and is similar to the FB-δ^{15}N of surface sediment from three other sites in the tropical/subtropical N. Atlantic (Figure 4c), and the bulk sedimentary δ^{15}N at the Cariaco Basin also reached a constant value after 5 ka [*Haug et al.*, 1998; *Meckler et al.*, 2007]. While requiring verification, this would seem to suggest that the last Holocene δ^{15}N decrease in the SCS record is not a global signal. The eastern equatorial north and south Pacific have distinctive features in their late Holocene δ^{15}N changes: most of the ETNP records show a continuous Holocene decrease in δ^{15}N [*Pride et al.*, 1999; *Emmer and Thunell*, 2000], while δ^{15}N in the ETSP levels off or even slightly increases in the late Holocene [*Martinez et al.*, 2006; *De Pol-Holz et al.*, 2006]. Considering the locations of these sites and circulation patterns, it is reasonable to suspect that the SCS is primarily influenced by denitrification in the ETNP, which could explain its continuous Holocene δ^{15}N decrease, whereas the isotopic signal of such regionally specific denitrifications would not survive into Caribbean Sea (e.g., the ETNP and ETSP late Holocene changes should partially cancel one another).

[32] The pre-deglacial δ^{15}N rise in the SCS may also be an imported regional isotopic signal. Although most records from the major denitrification zones show a δ^{15}N increase after the end of the last ice age, a few bulk sedimentary δ^{15}N records from the eastern equatorial Pacific suggest a δ^{15}N maximum starting at around 20 ka that is associated with a

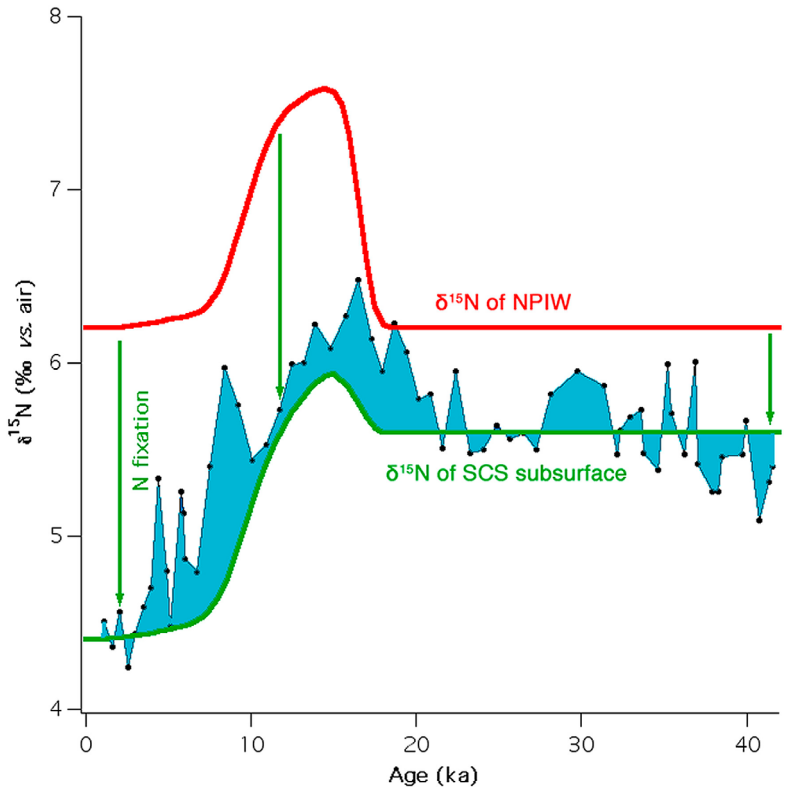

Figure 5. Conceptual illustration of the two mechanisms proposed to explain the basic δ^{15}N changes in the SCS FB-δ^{15}N records, as well as the aspects that call for additional processes. We assume minimal glacial/interglacial difference in NPIW nitrate δ^{15}N and a deglacial δ^{15}N maximum of ~1‰ (red curve). N fixation works to lower the δ^{15}N of nitrate in the thermocline of the SCS (green arrows), such that higher N fixation during the Holocene produces a larger δ^{15}N difference between NPIW nitrate (red curve) and the nitrate just below the euphotic zone in the SCS (green curve). We assume here that half of the N fixation increase occurs early in the deglaciation in response to increase in the water column denitrification, and the remaining N fixation increases more continuously through the deglaciation and Holocene in response to increasing sedimentary denitrification associated with sea level rise (using the simplified deglacial history of *Deutsch et al.* [2004]). The green line shows the trend expected from the combination of the mean ocean nitrate δ^{15}N and N fixation change. The data in black are the calculated subsurface δ^{15}N using the *G. ruber* FB-δ^{15}N record and the average δ^{15}N offset between the Holocene subsurface δ^{15}N and *G. ruber* FB-δ^{15}N of 0.4‰, such that the blue filled space indicates the deviation of subsurface δ^{15}N from the composite prediction based on mean ocean nitrate δ^{15}N and regional N fixation; the most important deviations are (1) the pre-deglacial component of the "deglacial" increase in FB-δ^{15}N, (2) the slowness of the decline in FB-δ^{15}N through the Holocene, (3) the single-sample FB-δ^{15}N maxima in the early Holocene that are shared by all three euphotic zone species. In the text, we describe several processes that may explain these deviations, which include changes in (i) water column denitrification in the eastern Pacific and (ii) the thermocline structure of the SCS.

regional increase in export production, suggesting a possible water column denitrification increase in the eastern equatorial Pacific prior to the last deglaciation [*Robinson et al.*, 2009]. This early rise in δ^{15}N, if introduced into the western equatorial Pacific by the NEC, might explain the early δ^{15}N increase in our SCS record. However, the cause for this early eastern Pacific δ^{15}N increase is not yet known, and it might also be interpreted as a local signal due to incomplete nitrate consumption [*Robinson et al.*, 2009]. Thus, it is a somewhat unsatisfying explanation for the early FB-δ^{15}N increase in the SCS.

[33] Pacific circulation changes in themselves may also affect the SCS record. The western Pacific is susceptible to several important modes of circulation change that might influence its communication with the eastern Pacific as well as the depth/thickness of the SCS thermocline, both of which could affect the δ^{15}N of shallow subsurface nitrate. In the context of a mid-Holocene δ^{15}N decrease observed in their record from near Mindanao (yellow curve in Figure 4b), *Kienast et al.* [2008] consider the possibilities of a mid-Holocene weakening of the NEC and/or a thickening of the western equatorial Pacific thermocline, tending to favor the latter. We have no further insight into the possibility of large scale western equatorial Pacific changes but simply note that the dynamics affecting the study region of *Kienast et al.* [2008] could also influence the SCS.

[34] As a marginal sea next to the Asian continent with its strong monsoonal system, the SCS in particular is sensitive

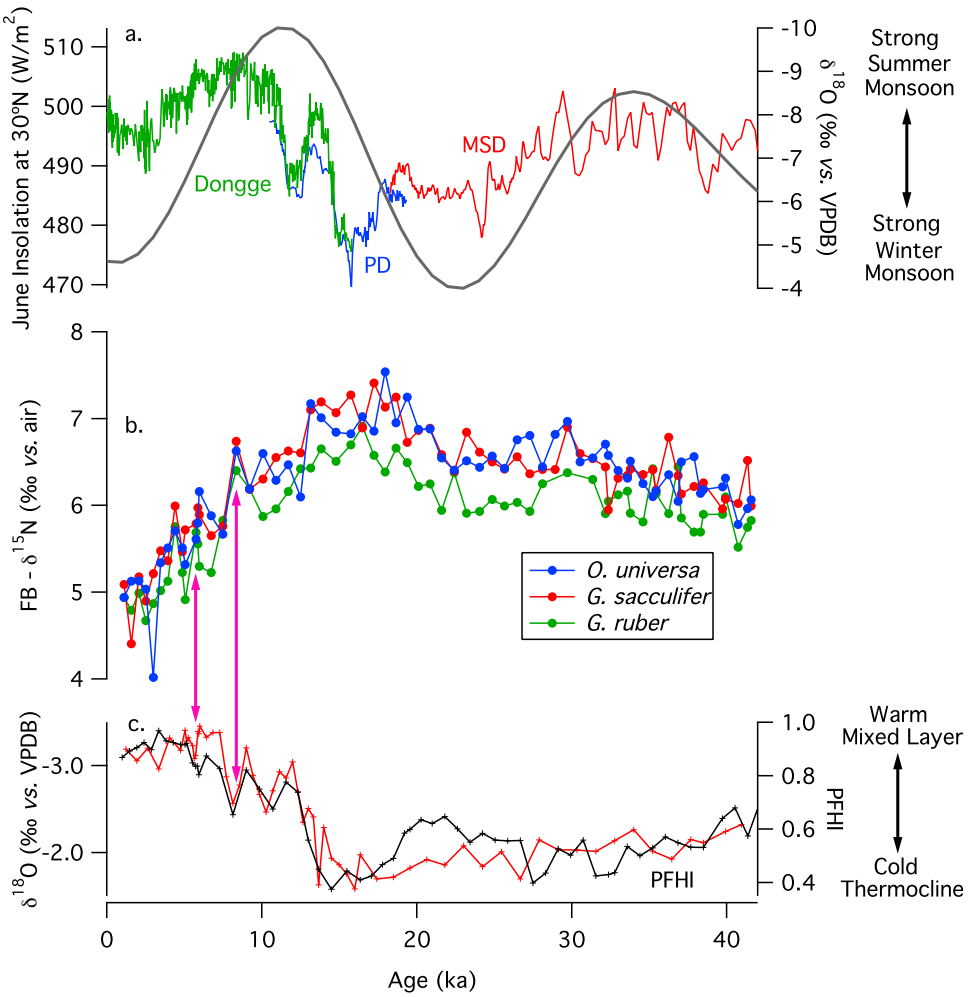

Figure 6. Comparison of the SCS FB-δ^{15}N records with other relevant paleoclimate data from the region. (a) June insolation at 30°N in gray, and cave records of East Asian monsoon variability in green, blue and red for different stalagmites [*Wang et al.*, 2001; *Dykoski et al.*, 2005]. (b) Planktonic FB-δ^{15}N of individual species from our study. (c) From the same sediments as Figure 6b, the δ^{18}O of *G. ruber* (white) calcite (‰ *vs.* VPDB) in red [*Wei et al.*, 2003], and planktonic foraminiferal hydrographic index (PFHI) in black [*Yu et al.*, 2006]. The latter is calculated as follows: PFHI = (% warm water species)/(%warm water species + %cold water species), where warm water species include *G. ruber* and *G. sacculifer*, and cold water species include *N. dutertrei* and *G. inflata.* Low PFHI suggests cold/upwelling conditions, while high PFHI suggests warm/stratified conditions. The purple arrows indicate periods of cold/shallow thermocline conditions that coincide with multispecies high FB-δ^{15}N events.

to changes in thermocline depth associated with wind changes. The SCS warmed slowly during deglaciation and through the Holocene [*Kienast et al.*, 2001; *Shintani et al.*, 2008], in contrast to the surrounding tropical western N. Pacific [*Rosenthal et al.*, 2003]. This difference is provisionally attributed to the effect of the monsoon cycle on the SCS [*Shintani et al.*, 2008]. Indeed, it is over the latter Holocene that cave records suggest a decline from the period of strong East Asian summer monsoon, under the influence of the ~20 kyr precessional cycle (Figure 6a) [*Wang et al.*, 2001; *Yuan et al.*, 2004]. In the SCS, the monsoon's effect, which apparently applied most strongly between 15 and 8 ka in the northern SCS [*Shintani et al.*, 2008], would have enhanced vertical exchange across the thermocline, weakening the vertical gradient in nitrate δ^{15}N and thus raising the δ^{15}N of the nitrate supply to the euphotic zone. This would have worked against the δ^{15}N decrease associated with deglacial increase in N fixation, effectively delaying the decline in SCS FB-δ^{15}N into the later Holocene. Moreover, if the deglacial-to-Holocene SCS thermocline changes varied neatly with the precessional cycle, this same hydrographic effect may also explain the rise in SCS FB-δ^{15}N before the onset of deglaciation, because of the increase in June insolation at ~22 ka (Figure 6). Stepping back from these specific speculations, variations in the East Asian monsoons could easily alter the timing of δ^{15}N changes away from the template three-step pattern of ice age, deglaciation, and Holocene.

[35] As described above, the Holocene has three brief FB-δ^{15}N maxima, typically defined by just a single depth but evident in all three euphotic zone species. These are found at approximate dates of 8.3 ka, 5.8 ka, and 4.4 ka

(Figure 6). Of these three events, the first at 8.3 ka clearly coincides with excursions in *G. ruber* δ^{18}O and the planktonic foraminifera hydrographic index (PFHI) [*Yu et al.*, 2006], both of which are consistent with these events involving cooling at the surface and/or a thermocline weakening (Figure 6; see caption for calculation of PFHI). This event may correspond with the well-described 8.2 ka cold event in Greenland [*Alley et al.*, 1997]. The second event also corresponds with smaller excursions in δ^{18}O and PFHI, but not as convincingly. Given the clear correspondences of the 8.3 ka FB-δ^{15}N maximum, we provisionally interpret all three of these events to be associated with hydrographic events driving upwelling and/or a weakening of the thermocline, which brought high δ^{15}N intermediate water closer to the surface and increased the δ^{15}N of shallow subsurface nitrate being mixed into the SCS euphotic zone. Given that the three events represent a significant part of the early to mid-Holocene record, their effect of increasing the mean δ^{15}N of the early Holocene may also be responsible for the general FB-δ^{15}N decrease into the later Holocene.

6. Conclusions and Future Work

[36] In this study, we use the δ^{15}N of the organic matter bound within the matrix of planktonic foraminiferal shells to reconstruct the changes in the δ^{15}N of the nitrate supply to the SCS euphotic zone over the last 42 ka. The FB-δ^{15}N record at the SCS, consistent among all analyzed planktonic foraminiferal species, shows a higher δ^{15}N during the last ice age than the current interglacial, and a deglacial maximum in δ^{15}N. Although global mean ocean nitrate δ^{15}N change is the likely driver of the deglacial δ^{15}N maximum in the SCS record, it is less likely to be the primary explanation for the glacial/interglacial difference in δ^{15}N. In any case, given that the glacial-to-interglacial FB-δ^{15}N decrease in the SCS is clearly smaller than that observed previously the Caribbean Sea, it rules out the possibility that the Caribbean δ^{15}N decrease was solely due to a mean ocean nitrate δ^{15}N decrease. Thus, the SCS data validate the interpretation of Caribbean data as indicating lower Atlantic N fixation during the last ice age [*Ren et al.*, 2009].

[37] The parallels between the SCS and the Caribbean Sea FB-δ^{15}N records suggest that N fixation is likely to be the common mechanism to account for the glacial/interglacial δ^{15}N difference in the tropical/subtropical oligotropic regions of both ocean basins. Together with reconstructions of water column denitrification, it supports the long-proposed importance of the response of N fixation to changes in the N inventory and N to P ratio in the ocean [*Redfield*, 1958; *Broecker*, 1982; *Tyrrell*, 1999]. While our data do not suggest iron as the dominant regulator of N fixation over the last glacial/interglacial cycle [e.g., *Falkowski*, 1997; *Broecker and Henderson*, 1998], neither the SCS nor Caribbean Sea are good candidates for iron limitation of N fixation [*Duce and Tindale*, 1991]. Future work in the central North Pacific or the South Pacific is needed to seek signs of glacial/interglacial changes in iron limitation on N fixers.

[38] Despite our growing evidence for reduced N fixation during the last ice age when denitrification was also reduced, we cannot yet exclude the possibility of changes in N inventory between last ice age and the current interglacial. As the balance in N budget is largely governed by the strength of the feedback between N fixation and denitrification, there are likely two ways to address the question in the future. First, the glacial/interglacial difference in mean ocean nitrate δ^{15}N and its time scale of response hold information regarding changes in the size of N inventory [*Deutsch et al.*, 2004]. While individual δ^{15}N records may be dominated by local processes such as denitrification, N fixation, and incomplete nitrate consumption, multiple records should eventually allow us differentiate global and regional prints. Second, the deglacial δ^{15}N changes in the SCS and Caribbean records might be used as model targets by which to evaluate the strength of the feedback between N fixation and denitrification and its implications for changes in N inventory.

[39] **Acknowledgments.** This study is a contribution to the Taiwan IMAGES project. Curation of the IMAGES core was conducted by the Core Laboratory under the National Center for Ocean Research. We thank Y. Wang for technical assistance, and two anonymous reviewers for their constructive comments. This work was supported by NSF grants OCE-0447570 and OPP-0453680 to D.M.S., by the Siebel Energy Grand Challenge of Princeton University, and by the Schlanger Ocean Drilling Program Fellowship and the Charlotte Elizabeth Procter Honorific Fellowship to H. R.

References

Alley, R. B., P. A. Mayewski, T. Sowers, M. Stuiver, K. C. Taylor, and P. U. Clark (1997), Holocene climatic instability: A prominent, widespread event 8200 yr ago, *Geology*, *25*(6), 483–486, doi:10.1130/0091-7613(1997)025<0483:HCIAPW>2.3.CO;2.

Altabet, M. A. (1988), Variations in nitrogen isotopic composition between sinking and suspended particles: Implications for nitrogen cycling and particle transformation in the open ocean, *Deep Sea Res., Part A*, *35*(4), 535–554.

Altabet, M. A., and R. Francois (1994), Sedimentary nitrogen isotopic ratio as a recorder for surface ocean nitrate utilization, *Global Biogeochem. Cycles*, *8*(1), 103–116, doi:10.1029/93GB03396.

Altabet, M. A., R. Francois, D. W. Murray, and W. L. Prell (1995), Climate-related variations in denitrification in the Arabian Sea from sediment $^{15}N/^{14}N$ ratios, *Nature*, *373*, 506–509, doi:10.1038/373506a0.

Altabet, M. A., C. Pilskaln, R. Thunell, C. Pride, D. Sigman, F. Chavez, and R. Francois (1999), The nitrogen isotope biogeochemistry of sinking particles from the margin of the eastern North Pacific, *Deep Sea Res., Part I*, *46*, 655–679, doi:10.1016/S0967-0637(98)00084-3.

Altabet, M. A., M. J. Higginson, and D. W. Murray (2002), The effect of millennial-scale changes in Arabian Sea denitrification on atmospheric CO_2, *Nature*, *415*(6868), 159–162, doi:10.1038/415159a.

Bassinot, F. C., L. D. Labeyrie, E. Vincent, X. Quidelleur, N. J. Shackleton, and Y. Lancelot (1994), The astronomical theory of climate and the age of the Brunhes Matuyama magnetic reversal, *Earth Planet. Sci. Lett.*, *126*, 91–108, doi:10.1016/0012-821X(94)90244-5.

Braman, R. S., and S. A. Hendrix (1989), Nanogram nitrite and nitrate determination in environmental and biological materials by V(III) reduction with chemiluminescence detection, *Anal. Chem.*, *61*, 2715–2718, doi:10.1021/ac00199a007.

Brandes, J. A., and A. H. Devol (2002), A global marine-fixed nitrogen isotopic budget: Implications for Holocene nitrogen cycling, *Global Biogeochem. Cycles*, *16*(4), 1120, doi:10.1029/2001GB001856.

Broecker, W. S. (1982), Glacial to interglacial changes in ocean chemistry, *Prog. Oceanogr.*, *11*, 151–197, doi:10.1016/0079-6611(82)90007-6.

Broecker, W. S., and G. M. Henderson (1998), The sequence of events surrounding Termination II and their implications for the cause of glacial-interglacial CO_2 changes, *Paleoceanography*, *13*(4), 352–364, doi:10.1029/98PA00920.

Broecker, W. S., et al. (1988), Accelerator mass spectrometry radiocarbon measurements on marine carbonate samples from deep sea cores and sediment traps, *Radiocarbon*, *30*(3), 261–295.

Broecker, W. S., T. H. Peng, S. Trumbore, G. Bonani, and W. Wolfli (1990), The distribution of radiocarbon in the glacial ocean, *Global Biogeochem. Cycles*, *4*(1), 103–117, doi:10.1029/GB004i001p00103.

Brunelle, B. G., D. M. Sigman, M. S. Cook, L. D. Keigwin, G. H. Haug, B. Plessen, G. Schettler, and S. L. Jaccard (2007), Evidence from diatom-bound nitrogen isotopes for subarctic Pacific stratification during the last ice age and a link to North Pacific denitrification changes, *Paleoceanography*, *22*, PA1215, doi:10.1029/2005PA001205.

Capone, D. G., J. P. Zehr, H. W. Paerl, B. Bergman, and F. J. Carpenter (1997), Trichodesmium, a globally significant marine cyanobacterium, *Science*, *276*, 1221–1229, doi:10.1126/science.276.5316.1221.

Carpenter, E. J., and C. C. Price (1977), Nitrogen fixation, distribution, and production of *Oscillatoria (Trichodesmium) spp.* in western Sargassso and Caribbean Seas, *Limnol. Oceanogr.*, *22*(1), 60–72, doi:10.4319/lo.1977.22.1.0060.

Casciotti, K. L., D. M. Sigman, M. G. Hastings, J. K. Bohlke, and A. Hilkert (2002), Measurement of the oxygen isotopic composition of nitrate in seawater and freshwater using the denitrifier method, *Anal. Chem.*, *74*(19), 4905–4912, doi:10.1021/ac020113w.

Chen, C.-T. A., S.-L. Wang, B.-J. Wang, and S.-C. Pai (2001), Nutrient budgets for the South China Sea basin, *Mar. Chem.*, *75*, 281–300, doi:10.1016/S0304-4203(01)00041-X.

Chen, C.-T. A., W.-P. Hou, T. Gamo, and S. L. Wang (2006), Carbonate-related parameters of subsurface waters in the West Philippine, South China and Sulu Seas, *Mar. Chem.*, *99*, 151–161, doi:10.1016/j.marchem.2005.05.008.

Chen, M.-T., L. Beaufort, and Shipboard Scientific Party of IMAGES III/MD106-IPHIS Cruise (Leg II) (1998), Exploring quaternary variability of the East Asia monsoon, Kuroshio current, and Western Pacific Warm Pool systems: High-resolution investigations of paleoceanography from the IMAGES III (MD106)-IPHIS Cruise, *Terr. Atmos. Oceanic Sci.*, *9*(1), 129–142.

Chen, Y.-L. L. (2005), Spatial and seasonal variations of nitrate-based new production and primary production in the South China Sea, *Deep Sea Res., Part I*, *52*, 319–340, doi:10.1016/j.dsr.2004.11.001.

Chen, Y.-L. L., H.-Y. Chen, and Y.-H. Lin (2003), Distribution and downward flux of *Trichodesmium* in the South China Sea as influenced by the transport from the Kuroshio Current, *Mar. Ecol. Prog. Ser.*, *259*, 47–57, doi:10.3354/meps259047.

Chen, Y.-L. L., H.-Y. Chen, D. M. Karl, and M. Takahashi (2004), Nitrogen modulates phytoplankton growth in spring in the South China Sea, *Cont. Shelf Res.*, *24*, 527–541, doi:10.1016/j.csr.2003.12.006.

Chen, Y.-L. L., H.-Y. Chen, S.-H. Tuo, and K. Ohki (2008), Seasonal dynamics of new production from *Trichodesmium* N_2 fixation and nitrate uptake in the upstream Kuroshio and South China Sea basin, *Limnol. Oceanogr.*, *53*(5), 1705–1721, doi:10.4319/lo.2008.53.5.1705.

Christensen, J. P. (1994), Carbon export from continental shelves, denitrification and atmospheric carbon dioxide, *Cont. Shelf Res.*, *14*, 547–576, doi:10.1016/0278-4343(94)90103-1.

De Pol-Holz, R., O. Ulloa, L. Dezileau, J. Kaiser, F. Lamy, and D. Hebbeln (2006), Melting of the Patagonian Ice Sheet and deglacial perturbations of the nitrogen cycle in the eastern South Pacific, *Geophys. Res. Lett.*, *33*, L04704, doi:10.1029/2005GL024477.

De Pol-Holz, R., O. Ulloa, F. Lamy, L. Dezileau, P. Sabatier, and D. Hebbeln (2007), Late Quaternary variability of sedimentary nitrogen isotopes in the eastern South Pacific Ocean, *Paleoceanography*, *22*, PA2207, doi:10.1029/2006PA001308.

Deutsch, C., D. M. Sigman, R. C. Thunell, N. Meckler, and G. H. Haug (2004), Stable isotope constraints on the glacial/interglacial oceanic nitrogen budget, *Global Biogeochem. Cycles*, *18*, GB4012, doi:10.1029/2003GB002189.

Deutsch, C., J. L. Sarmiento, D. M. Sigman, N. Gruber, and J. P. Dunne (2007), Spatial coupling of nitrogen inputs and losses in the ocean, *Nature*, *445*(7124), 163–167, doi:10.1038/nature05392.

Duce, R. A., and N. W. Tindale (1991), Atmospheric transport of iron and its deposition in the ocean, *Limnol. Oceanogr.*, *36*(8), 1715–1726, doi:10.4319/lo.1991.36.8.1715.

Dugdale, R. C., and J. J. Goering (1967), Uptake of new and regenerated forms of nitrogen in primary productivity, *Limnol. Oceanogr.*, *12*(2), 196–206, doi:10.4319/lo.1967.12.2.0196.

Dykoski, C. A., R. L. Edwards, H. Cheng, D. X. Yuan, Y. J. Cai, M. L. Zhang, Y. S. Lin, J. M. Qing, Z. S. An, and J. Revenaugh (2005), A high-resolution, absolute-dated Holocene and deglacial Asian monsoon record from Dongge Cave, China, *Earth Planet. Sci. Lett.*, *233*, 71–86, doi:10.1016/j.epsl.2005.01.036.

Emmer, E., and R. C. Thunell (2000), Nitrogen isotope variations in Santa Barbara Basin sediments: Implications for denitrification in the eastern tropical North Pacific during the last 50,000 years, *Paleoceanography*, *15*(4), 377–387, doi:10.1029/1999PA000417.

Falkowski, P. G. (1997), Evolution of the nitrogen cycle and its influence on the biological sequestration of CO_2 in the ocean, *Nature*, *387*(6630), 272–275, doi:10.1038/387272a0.

Galbraith, E. D., M. Kienast, S. L. Jaccard, T. F. Pedersen, B. G. Brunelle, D. M. Sigman, and T. Kiefer (2008), Consistent relationship between global climate and surface nitrate utilization in the western subarctic Pacific throughout the last 500 ka, *Paleoceanography*, *23*, PA2212, doi:10.1029/2007PA001518.

Ganeshram, R. S., T. F. Pedersen, S. E. Calvert, and J. W. Murray (1995), Large changes in oceanic nutrient inventories from glacial to interglacial periods, *Nature*, *376*, 755–758, doi:10.1038/376755a0.

Ganeshram, R. S., T. F. Pedersen, S. E. Calvert, G. W. McNeill, and M. R. Fontugne (2000), Glacial-interglacial variability in denitrification in the world's oceans: Causes and consequences, *Paleoceanography*, *15*(4), 361–376, doi:10.1029/1999PA000422.

Ganeshram, R. S., T. F. Pedersen, S. E. Calvert, and R. Francois (2002), Reduced nitrogen fixation in the glacial ocean inferred from changes in marine nitrogen and phosphorus inventories, *Nature*, *415*, 156–159, doi:10.1038/415156a.

Gaye, B., M. G. Wiesner, and N. Lahajnar (2009), Nitrogen sources in the South China Sea, as discerned from stable nitrogen isotopic ratios in rivers, sinking particles, and sediments, *Mar. Chem.*, *114*, 72–85, doi:10.1016/j.marchem.2009.04.003.

Haug, G. H., T. F. Pedersen, D. M. Sigman, S. E. Calvert, B. Nielsen, and L. C. Peterson (1998), Glacial/interglacial variations in production and nitrogen fixation in the Cariaco Basin during the last 580 kyr, *Paleoceanography*, *13*, 427–432, doi:10.1029/98PA01976.

Higginson, M. J., J. R. Maxwell, and M. A. Altabet (2003), Nitrogen isotope and chlorin paleoproductivity records from the Northern South China Sea: Remote vs. local forcing of millennial- and orbital-scale variability, *Mar. Geol.*, *201*, 223–250, doi:10.1016/S0025-3227(03)00218-4.

Kao, S.-J., K.-K. Liu, S.-C. Hsu, Y.-P. Chang, and M. H. Dai (2008), North Pacific-wide spreading of isotopically heavy nitrogen during the last deglaciation: Evidence from the western Pacific, *Biogeosciences*, *5*(6), 1641–1650, doi:10.5194/bg-5-1641-2008.

Karl, D., A. Michaels, B. Bergman, D. Capone, E. Carpenter, R. Letelier, F. Lipschultz, H. Paerl, D. Sigman, and L. Stal (2002), Dinitrogen fixation in the world's oceans, *Biogeochemistry*, *57*, 47–98, doi:10.1023/A:1015798105851.

Kienast, M. (2000), Unchanged nitrogen isotopic composition of organic matter in the South China Sea during the last climatic cycle: Global implications, *Paleoceanography*, *15*(2), 244–253, doi:10.1029/1999PA000407.

Kienast, M., S. Steinke, K. Stattegger, and S. E. Calvert (2001), Synchronous tropical South China Sea SST change and Greenland warming during deglaciation, *Science*, *291*, 2132–2134, doi:10.1126/science.1057131.

Kienast, M., M. J. Higginson, G. Mollenhauer, T. I. Eglinton, M.-T. Chen, and S. E. Calvert (2005), On the sedimentological origin of down-core variations of bulk sedimentary nitrogen isotope ratios, *Paleoceanography*, *20*, PA2009, doi:10.1029/2004PA001081.

Kienast, M., M. F. Lehmann, A. Timmermann, E. Galbraith, T. Bolliet, A. Holbourn, C. Normandeau, and C. Laj (2008), A mid-Holocene transition in the nitrogen dynamics of the western equatorial Pacific: Evidence of a deepening thermocline?, *Geophys. Res. Lett.*, *35*, L23610, doi:10.1029/2008GL035464.

Knapp, A. N., D. M. Sigman, and F. Lipschultz (2005), N isotopic composition of dissolved organic nitrogen and nitrate at the Bermuda Atlantic time-series study site, *Global Biogeochem. Cycles*, *19*, GB1018, doi:10.1029/2004GB002320.

Knapp, A. N., P. J. DiFiore, C. Deutsch, D. M. Sigman, and F. Lipschultz (2008), Nitrate isotopic composition between Bermuda and Puerto Rico: Implications for N-2 fixation in the Atlantic Ocean, *Global Biogeochem. Cycles*, *22*, GB3014, doi:10.1029/2007GB003107.

Lin, L.-L., and H.-Y. Hsieh (2007), Seasonal variations of modern planktonic foraminifera in the South China Sea, *Deep Sea Res., Part II*, *54*, 1634–1644, doi:10.1016/j.dsr2.2007.05.007.

Liu, K. K., M. J. Su, C. R. Hsueh, and G. C. Gong (1996), The nitrogen isotopic composition of nitrate in the Kuroshio Water northeast of Taiwan: Evidence for nitrogen fixation as a source of isotopically light nitrate, *Mar. Chem.*, *54*, 273–292, doi:10.1016/0304-4203(96)00034-5.

Liu, K.-K., S.-Y. Chao, P.-T. Shaw, G.-C. Gong, C.-C. Chen, and T. Y. Tang (2002), Monsoon-forced chlorophyll distribution and primary production in the South China Sea: Observations and a numerical study, *Deep Sea Res., Part I*, *49*, 1387–1412, doi:10.1016/S0967-0637(02)00035-3.

Loick, N., J. Dippner, H. N. Doan, I. Liskow, and M. Voss (2007), Pelagic nitrogen dynamics in the Vietnamese upwelling area according to stable nitrogen and carbon isotope data, *Deep Sea Res., Part I*, *54*, 596–607, doi:10.1016/j.dsr.2006.12.009.

Martinez, P., F. Lamy, R. R. Robinson, L. Pichevin, and I. Billy (2006), Atypical δ^{15}N variations at the southern boundary of the East Pacific oxygen minimum zone over the last 50 ka, *Quat. Sci. Rev.*, *25*, 3017–3028, doi:10.1016/j.quascirev.2006.04.009.

McElroy, M. B. (1983), Marine biological-controls on atmospheric CO_2 and climate, *Nature*, *302*, 328–329, doi:10.1038/302328a0.

Meckler, A. N., G. H. Haug, D. M. Sigman, B. Plessen, L. C. Peterson, and H. R. Thierstein (2007), Detailed sedimentary N isotope records from Cariaco Basin for Terminations I and V: Local and global implications, *Global Biogeochem. Cycles*, *21*, GB4019, doi:10.1029/2006GB002893.

Mehra, O. P., and M. L. Jackson (1958), Iron oxide removal from soils and clays by a dithionite-citrate system buffered with sodium bicarbonate, *Clays Clay Miner.*, *7*, 317–327, doi:10.1346/CCMN.1958.0070122.

Montoya, J. P., P. H. Wiebe, and J. J. McCarthy (1992), Natural abundance of ^{15}N in particulate nitrogen and zooplankton in the Gulf Stream region and warm core ring 86A, *Deep Sea Res., Part A*, *39*, 363–392.

Montoya, J. P., E. J. Carpenter, and D. G. Capone (2002), Nitrogen fixation and nitrogen isotope abundances in zooplankton of the oligotrophic North Atlantic, *Limnol. Oceanogr.*, *47*(6), 1617–1628, doi:10.4319/lo.2002.47.6.1617.

Nydahl, F. (1978), Peroxodisulfate oxidation of total nitrogen in waters to nitrate, *Water Res.*, *12*, 1123–1130, doi:10.1016/0043-1354(78)90060-X.

Pride, C., R. Thunell, D. M. Sigman, L. Keigwin, M. Altabet, and E. Tappa (1999), Nitrogen isotopic variations in the Gulf of California since the Last Deglaciation: Response to global climate change, *Paleoceanography*, *14*(3), 397–409, doi:10.1029/1999PA900004.

Rafter, P. A., D. M. Sigman, C. D. Charles, J. Kaiser, and G. H. Haug (2012), Subsurface tropical Pacific nitrogen isotopic composition of nitrate: Biogeochemical signals and their transport, *Global Biogeochem. Cycles*, *26*, GB1003, doi:10.1029/2010GB003979.

Ravelo, A. C., and R. G. Fairbanks (1992), Oxygen isotopic composition of multiple species of planktonic foraminifera: Recorders of the modern photic zone temperature gradient, *Paleoceanography*, *7*, 815–831, doi:10.1029/92PA02092.

Redfield, A. C. (1958), The biological control of chemical factors in the environment, *Am. Sci.*, *46*, 205–221.

Ren, H., D. M. Sigman, A. N. Meckler, B. Plessen, R. S. Robinson, Y. Rosenthal, and G. H. Haug (2009), Foraminiferal isotope evidence of reduced nitrogen fixation in the ice age Atlantic Ocean, *Science*, *323*(5911), 244–248, doi:10.1126/science.1165787.

Ren, H., D. M. Sigman, R. Thunell, and M. G. Propopenko (2012), Nitrogen isotopic composition of planktonic foraminifera from the modern ocean and recent sediments, *Limnol. Oceanogr.*, in press.

Robinson, R., A. Mix, and P. Martinez (2007), Southern Ocean control on the extent of denitrification in the southeast Pacific over the last 70 ka, *Quat. Sci. Rev.*, *26*(1–2), 201–212, doi:10.1016/j.quascirev.2006.08.005.

Robinson, R. S., P. Martinez, L. D. Pena, and I. Cacho (2009), Nitrogen isotopic evidence for deglacial changes in nutrient supply in the eastern equatorial Pacific, *Paleoceanography*, *24*, PA4213, doi:10.1029/2008PA001702.

Rosenthal, Y., D. W. Oppo, and B. K. Linsley (2003), The amplitude and phasing of climate change during the last deglaciation in the Sulu Sea, western equatorial Pacific, *Geophys. Res. Lett.*, *30*(8), 1428, doi:10.1029/2002GL016612.

Schindler, D. W. (1977), Evolution of phosphorus limitation in lakes, *Science*, *195*(4275), 260–262, doi:10.1126/science.195.4275.260.

Schubert, C. J., and S. E. Calvert (2001), Nitrogen and carbon isotopic composition of marine and terrestrial organic matter in Arctic Ocean sediments: Implications for nutrient utilization and organic matter composition, *Deep Sea Res., Part I*, *48*(3), 789–810, doi:10.1016/S0967-0637(00)00069-8.

Shintani, T., M. Yamamoto, and M.-T. Chen (2008), Slow warming of the northern South China Sea during the last deglaciation, *Terr. Atmos. Oceanic Sci.*, *19*(4), 341–346, doi:10.3319/TAO.2008.19.4.341(IMAGES).

Shiozaki, T., K. Furuya, T. Kodama, S. Kitajima, S. Takeda, T. Takemura, and J. Kanda (2010), New estimation of N_2 fixation in the western and central Pacific Ocean and its marginal seas, *Global Biogeochem. Cycles*, *24*, GB1015, doi:10.1029/2009GB003620.

Sigman, D. M., M. A. Altabet, D. C. McCorkle, R. Francois, and G. Fisher (2000), The δ^{15}N of nitrate in the Southern Ocean: Nitrogen cycling and circulation in the ocean interior, *J. Geophys. Res.*, *105*(C8), 19,599–19,614, doi:10.1029/2000JC000265.

Sigman, D. M., K. L. Casciotti, M. Andreani, C. Barford, M. Galanter, and J. K. Bohlke (2001), A bacterial method for the nitrogen isotopic analysis of nitrate in seawater and freshwater, *Anal. Chem.*, *73*(17), 4145–4153, doi:10.1021/ac010088e.

Sigman, D. M., P. J. DiFiore, M. P. Hain, C. Deutsch, and D. M. Karl (2009), Sinking organic matter spreads the nitrogen isotope signal of pelagic denitrification in the North Pacific, *Geophys. Res. Lett.*, *36*, L08605, doi:10.1029/2008GL035784.

Sverdrup, H. U., M. W. Johnson, and R. H. Fleming (1942), *The Oceans: Their Physics, Chemistry, and General Biology*, 1087 pp., Prentice-Hall, Englewood Cliffs, N. J.

Tamburini, F., T. Adatte, K. Follmi, S. M. Bernasconi, and P. Steinmann (2003), Investigating the history of East Asian monsoon and climate during the last glacial-interglacial period (0–140000 years): Mineralogy and geochemistry of ODP Sites 1143 and 1144, South China Sea, *Mar. Geol.*, *201*, 147–168, doi:10.1016/S0025-3227(03)00214-7.

Thunell, R. C., Q. Miao, S. E. Calvert, and T. F. Pedersen (1992), Glacial-Holocene biogenic sedimentation patterns in the South China Sea: Productivity variations and surface water pCO_2, *Paleoceanography*, *7*(2), 143–162, doi:10.1029/92PA00278.

Tyrrell, T. (1999), The relative influences of nitrogen and phosphorus on oceanic primary production, *Nature*, *400*, 525–531, doi:10.1038/22941.

Uhle, M. E., S. A. Macko, H. J. Spero, M. H. Engel, and D. W. Lea (1997), Sources of carbon and nitrogen in modern planktonic foraminifera: The role of algal symbionts as determined by bulk and compound specific stable isotopic analyses, *Org. Geochem.*, *27*(3–4), 103–113, doi:10.1016/S0146-6380(97)00075-2.

Wada, E., and A. Hattori (1976), Natural abundance of ^{15}N in particulate organic matter in North Pacific Ocean, *Geochim. Cosmochim. Acta*, *40*(2), 249–251, doi:10.1016/0016-7037(76)90183-6.

Wang, Y. J., H. Cheng, R. L. Edwards, Z. S. An, J. Y. Wu, C.-C. Shen, and J. A. Dorale (2001), A high-resolution absolute-dated late Pleistocene Monsoon record from Hulu Cave, China, *Science*, *294*, 2345–2348, doi:10.1126/science.1064618.

Wang, R. J., Z. M. Jian, W. S. Xiao, J. Tian, J. R. Li, R. H. Chen, Y. L. Zheng, and J. F. Chen (2007), Quaternary biogenic opal records in the South China Sea: Linkages to East Asian monsoon, global ice volume and orbital forcing, *Sci. China, Ser. D Earth Sci.*, *50*(5), 710–724.

Wei, K.-Y., T.-C. Chiu, and Y.-G. Chen (2003), Toward establishing a maritime proxy record of the East Asian summer monsoons for the late Quaternary, *Mar. Geol.*, *201*, 67–79, doi:10.1016/S0025-3227(03)00209-3.

Winckler, G., R. F. Anderson, M. Q. Fleisher, D. McGee, and N. Mahowald (2008), Covariant glacial-interglacial dust fluxes in the equatorial Pacific and Antarctica, *Science*, *320*, 93–96, doi:10.1126/science.1150595.

Wong, G. T. F., S.-W. Chung, F.-K. Shiah, C.-C. Chen, L.-S. Wen, and K.-K. Liu (2002), Nitrate anomaly in the upper nutricline in the northern South China Sea—Evidence for nitrogen fixation, *Geophys. Res. Lett.*, *29*(23), 2097, doi:10.1029/2002GL015796.

Wong, G. T. F., C.-M. Tseng, L.-S. Wen, and S.-W. Chung (2007), Nutrient dynamics and N-anomaly at the SEATS station, *Deep Sea Res., Part II*, *54*, 1528–1545, doi:10.1016/j.dsr2.2007.05.011.

You, Y. (2003), The pathway and circulation of North Pacific Intermediate Water, *Geophys. Res. Lett.*, *30*(24), 2291, doi:10.1029/2003GL018561.

Yu, P.-S., C.-C. Huang, Y. Chin, H.-S. Mii, and M.-T. Chen (2006), Late Quaternary East Asian Monsoon variability in the South China Sea: Evidence from planktonic foraminifera faunal and hydrographic gradient records, *Palaeogeogr. Palaeoclimatol. Palaeoecol.*, *236*, 74–90, doi:10.1016/j.palaeo.2005.11.038.

Yuan, D. X., et al. (2004), Timing, duration, and transitions of the Last Interglacial Asian Monsoon, *Science*, *304*(5670), 575–578, doi:10.1126/science.1091220.

M.-T. Chen, Institute of Applied Geophysics, National Taiwan Ocean University, Keelung 20224, Taiwan.

S.-J. Kao, Research Center for Environmental Changes, Academia Sinica, Taipei 115, Taiwan.

H. Ren, Lamont-Doherty Earth Observatory, Palisades, NY 10964, USA. (hren@ldeo.columbia.edu)

D. M. Sigman, Department of Geosciences, Princeton University, Guyot Hall, Princeton, NJ 08544, USA.